Polymer Chemistry

PAPER

View Article Online
View Journal | View Issue

Cite this: *Polym. Chem.*, 2015, **6**, 5693

On the structure–control relationship of amide-functionalized SG1-based alkoxyamines for nitroxide-mediated polymerization and conjugation†

Elise Guégain,[a] Vianney Delplace,[a] Thomas Trimaille,[b] Didier Gigmes,[b] Didier Siri,[b] Sylvain R. A. Marque,[b] Yohann Guillaneuf[b] and Julien Nicolas*[a]

Received 22nd February 2015,
Accepted 19th March 2015

DOI: 10.1039/c5py00283d

www.rsc.org/polymers

The functionalization of alkoxyamines prior to nitroxide-mediated polymerization (NMP) induces important structural variations when compared to the parent molecules. This may have important consequences on the design of functionalized materials by pre-functionalization. In this context, a wide range of amide-functionalized alkoxyamines (a functionality often obtained after conjugation from COOH– and *N*-succinimidyl-containing alkoxyamines) based on the nitroxide SG1 (*N*-*tert*-butyl-*N*-(1-diethyl phosphono-2,2-dimethylpropyl) nitroxide) have been synthesized and their dissociation rate constants (k_d) have been determined. To rationalize their reactivity, a multi-parameter procedure was applied and enabled to discriminate disubstituted amide-functionalized alkoxyamines from monosubstituted ones. Monosubstituted alkoxyamines exhibited lower k_d than their disubstituted counterparts (E_a increase of ~7–10 kJ mol^{-1}) because of the occurrence of intramolecular hydrogen bonding (IHB) between the alkyl and the nitroxide fragments. NMP of styrene, *n*-butyl acrylate and methyl methacrylate with a small amount of acrylonitrile was then successfully performed from two representative secondary SG1-based alkoxyamines employed for conjugation: namely AMA (COOH-containing) and AMA-NHS (*N*-succinimidyl derivative), and compared to polymerizations initiated with AMA-Gem, an AMA-based alkoxyamine pre-functionalized with the anticancer drug Gemcitabine (Gem) and subjected to IHB. Although AMA-NHS showed the best results due to its lower E_a, the strong polarity of the Gem moiety that counter-balanced the detrimental effect of IHB over its k_d still allowed for a reasonable control.

Introduction

Nitroxide-mediated polymerization (NMP),[1,2] atom-transfer radical polymerization (ATRP)[3,4] and reversible addition–fragmentation chain transfer (RAFT)[5,6] polymerization – to mention only the most popular – are very efficient reversible deactivation radical polymerization (RDRP) techniques. Over the last few decades, the field of macromolecular synthesis has been revolutionized as designing well-defined, complex and functional architectures is now possible with great ease. The use of a preformed alkoxyamine,[1] a 2-in-1 molecule which undergoes reversible thermal homolysis to produce an initiating radical and a persistent nitroxide, is definitely the most efficient procedure to perform NMP. The NMP mechanism is governed by a reversible activation–deactivation equilibrium where the nitroxide reversibly deactivates the growing radicals into dormant alkoxyamine functionalities (Scheme 1a).[1,7]

Among the features of NMP that benefitted from recent developments is the ease of access to functionalized alkoxyamines for (bio)conjugation purposes.[1] For instance, carboxylic acid-containing SG1-based alkoxyamines, such as the Bloc-Builder alkoxyamine (2-methyl-2-(*N*-*tert*-butyl-*N*-(1-diethoxyphosphoryl-2,2-dimethylpropyl)aminoxy) propionic acid) or its secondary counterpart, the AMA-SG1 (2-(*N*-*tert*-butyl-*N*-(1-diethoxyphosphoryl-2,2-dimethylpropyl)aminoxy) propionic acid) alkoxyamine (Scheme 1b), enabled coupling with primary amines. This is achieved either after their conversion into the corresponding *N*-succinimidyl (NHS) ester derivative[8–10] or

[a]*Institut Galien Paris-Sud, CNRS UMR 8612, Univ. Paris-Sud, Faculté de Pharmacie, 5 rue Jean-Baptiste Clément, F-92296 Châtenay-Malabry cedex, France. E-mail: julien.nicolas@u-psud.fr; https://twitter.com/julnicolas; Fax: +33 1 46 83 55 11; Tel: +33 1 46 83 58 53*
[b]*Aix-Marseille University CNRS UMR 7273, Institut de Chimie Radicalaire, Avenue Escadrille Normandie-Niemen, 13397 Marseille Cedex 20, France*
†Electronic supplementary information (ESI) available. See DOI: 10.1039/c5py00283d

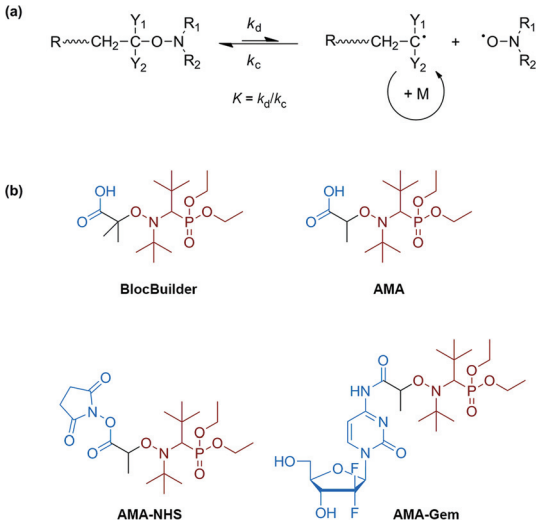

Scheme 1 General scheme of the NMP mechanism with k_c = combination rate constant, k_d = dissociation rate constant and K = activation–deactivation equilibrium constant (a). Structures of the BlocBuilder, AMA, AMA-NHS and AMA-Gem SG1-based alkoxyamines (b).

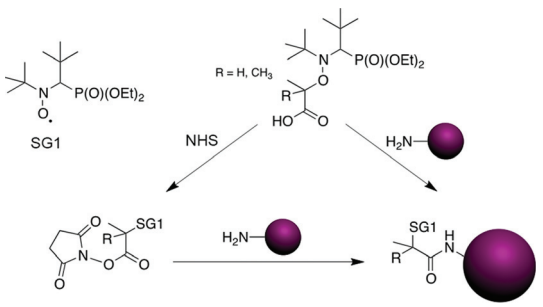

Scheme 2 Functionalization of SG1-based alkoxyamines *via* an amide linkage.

through their direct use in combination with benzotriazol-1-yloxytripyrrolidinophosphonium hexafluorophosphate (PyBOP) as a coupling agent (Scheme 2).[11,12]

In particular, these NHS-based alkoxyamines were employed for the linkage of preformed NHS-functional PEG-based polymers to a protein[9] whereas PyBOP was used for the direct coupling of the alkoxyamine to the terminal amine group of a peptide through solid-phase peptide synthesis[11] or to an anticancer drug,[12] prior to performing NMP. This last strategy, which can be assimilated to a "*grafting from*" approach in the case of bulky substrates, exhibits two main benefits compared to the reverse strategy involving the coupling of preformed α-functional polymers (generally termed "*grafting to*"): (i) the efficiency of the conjugation is generally higher, especially for bulky substrates, due to a lower steric hindrance and (ii) the purification of the resulting conjugates is facilitated as only the unreacted monomer has to be removed. However, pre-functionalizing alkoxyamines induces important structural changes when compared to the parent molecules. In particular, all pre-functionalized SG1-based alkoxyamines employed for (bio)conjugation so far have amide functionalities whereas the parent BlocBuilder and AMA alkoxyamines have a carboxylic acid group (see Scheme 2). Since the dissociation rate constant (k_d) of the alkoxyamine is governed by the structure of the alkyl moiety, with a combination of polar, steric and stabilization effects,[13] such structural modifications are likely to impact their dissociation. This is of high importance since, for a given monomer and nitroxide, the k_d value determines the degree of control over the polymerization.[14] Therefore, pre-functionalization of alkoxyamines could alter their controlling ability compared to that of non-functionalized counterparts.

This context prompted us to first investigate the reactivity of a series of functionalized amide-containing alkoxyamines based on the SG1 nitroxide and deriving from the BlocBuilder or the AMA alkoxyamines to determine whether their radical reactivity was influenced by the functionalization. In a second step, NMP of representative monomers (*i.e.*, styrene, *n*-butyl acrylate and methyl methacrylate with a small amount of acrylonitrile) was achieved from a selection of alkoxyamines to illustrate our findings. We selected three secondary SG1-based alkoxyamines (they usually give higher coupling yields due to their less hindered structures compared to tertiary analogs),[9,15] which can find application in the "*grafting from*" strategy (Scheme 2): (i) the AMA alkoxyamine, bearing a carboxylic group; (ii) its NHS derivative (AMA-NHS); and (iii) an amide-functionalized alkoxyamine bearing the anticancer drug Gemcitabine (AMA-Gem, Scheme 1), synthesized by the direct coupling between AMA and Gemcitabine. The main idea was to perform point-by-point comparisons between these three alkoxyamines to highlight the potential influence of the functionalization over the polymerization. Comparing AMA, AMA-NHS and AMA-Gem gave indications about structure–control relationship for each class of monomer and helped to predict their behavior for the design of functional materials depending on the grafting strategy (*i.e.*, "*grafting from*" *vs.* "*grafting to*"). Note that AMA-Gem is of high interest as we recently showed that the controlled growth of short polyisoprene chains from this alkoxyamine enabled the resulting amphiphilic species to self-assemble into stable, narrowly dispersed nanoparticles of 130–160 nm in diameter with significant *in vivo* anticancer activity on human pancreatic carcinoma-bearing mice.[12] Considering the great potential of this strategy, an in-depth investigation of the behavior and the controlling ability of AMA-Gem towards different monomer families is of high importance to design well-defined functionalized materials for anticancer applications.

Experimental part

Materials

2-Methoxyethylamine (99%), *tert*-butylamine (98%), *N*-isopropylacrylamide (>99%), CuBr (98%), copper powder (<10 microns, 99%), 2-bromo propionic acid (99%), *N*,*N*,*N*′,*N*″,*N*″-pentamethyldiethylenetriamine (PMDETA, 99%), *N*,*N*′-

dicyclohexylcarbodiimide (DCC, 99%), *N*,*N*-diisopropylethylamine (DIPEA, 99%) and (benzotriazol-1-yloxy)tripyrrolidinophosphonium hexafluorophosphate (PyBOP, 98%) were purchased from Aldrich. *N*-Hydroxysuccinimide (NHS, 98%) was supplied by Acros and Gemcitabine hydrochloride (Gem HCl) from Sequoia Research Products Limited. Styrene (S, 99%), *n*-butyl acrylate (*n*BA, 99%), methyl methacrylate (MMA, 99%), and acrylonitrile (AN, 99+%) were purchased from Aldrich and were used as received (except for MMA which was distilled). Deuterated chloroform ($CDCl_3$) was obtained from Euristop. Dry dimethylformamide (DMF) and dry toluene were obtained from Aldrich and all other solvents were purchased from Carlo Erba. *N*-*tert*-Butyl-*N*-(1-diethyl phosphono-2,2-dimethylpropyl) nitroxide (SG1, 86%) and BlocBuilder MA **1** were kindly supplied by Arkema. The *O*-acetylated-glucosamine was synthesized as described in ref. 16. 2-Bromo-*N*,*N*-dimethylpropanamide and 2-bromo-*N*-isopropylpropanamide were prepared as described in ref. 17. 2-Bromo-2-methyl-*N*,*N*-dimethylpropanamide was prepared as described in ref. 18. Alkoxyamine **2** was prepared as described in ref. 19. Alkoxyamine **3b** was prepared as described in ref. 20. Alkoxyamine **4** was prepared as described in ref. 11. Alkoxyamines **13–15** were prepared as described in ref. 21. 2-[*N*-*tert*-Butyl-*N*-(1-diethoxyphosphoryl-2,2-dimethylpropyl)aminoxy]-propionic acid (AMA, **8**),[22] 2-[*N*-*tert*-butyl-*N*-(1-diethoxyphosphoryl-2,2-dimethylpropyl)aminoxy]-*N*-propionyloxysuccinimide (AMA-NHS, **11**),[9] and AMA-Gem **12**[12] were synthesized according to previously reported methods. Note that for AMA, an enhancement of crystallization is performed by dissolving the colorless oil in 1 mL of ethyl acetate followed by coevaporation of both ethyl acetate and residual dichloromethane (DCM) under vacuum. For AMA-NHS alkoxyamine, only the major diastereoisomer was obtained.

Analytical techniques

^{1}H NMR spectroscopy was performed in 5 mm diameter tubes in $CDCl_3$ on a Bruker Avance-300 (300 MHz) spectrometer. The chemical shift scale was calibrated on the basis of the solvent peak (δ = 7.26 ppm). ^{13}C NMR spectroscopy was performed in 5 mm diameter tubes in $CDCl_3$ on a Bruker Avance-300 (75 MHz) spectrometer. The chemical shift scale was calibrated on the basis of the solvent peak (δ = 77.0 ppm). Size exclusion chromatography (SEC) was performed at 30 °C with two columns from Polymer Laboratories (PL-gel MIXED-D; 300 × 7.5 mm; bead diameter, 5 μm; linear part, 400–4 × 10^5 g mol^{-1}) and a differential refractive index detector (Spectrasystem RI-150 from Thermo Electron Corp.), using chloroform ($CHCl_3$) as an eluent, a Waters 515 pump at a flow rate of 1 mL min^{-1}, and toluene as a flow-rate marker. The conventional calibration curve was based on poly(methyl methacrylate) (PMMA) standards (peak molar masses, M_p = 625–625 500 g mol^{-1}) or polystyrene (PS) standards[23] (peak molar masses, M_p = 162–523 000 g mol^{-1}) from Polymer Laboratories. This technique allowed M_n (number-average molar mass), M_w (weight-average molar mass), and M_w/M_n (dispersity, $Đ$) to be determined.

Methods

Synthesis of SG1-based alkoxyamines

Alkoxyamine 3a. 2-Methoxyethylamine (0.75 mL, 8.6 mmol) was added through a syringe to a solution of BlocBuilder-NHS alkoxyamine (2 g, 4.2 mmol) in DCM (100 mL) at 0 °C under an inert atmosphere. After 1 h under stirring, the reaction mixture was concentrated under reduced pressure until a white gum was obtained. The latter was washed with distilled water, dissolved in DCM and poured into cold pentane. After filtration of the insoluble part (several milligrams), the filtrate was placed at −20 °C overnight. The white gum formed in the bottom of the flask was separated from pentane by removing the latter with a pipette. The product was briefly washed with cold pentane, and dried under vacuum. Yield: 55% (1.01 g). ^{1}H NMR ($CDCl_3$, δ, ppm): 1.12 (s, 9H), 1.19 (s, 9H), 1.34 (m, 6H), 1.60 (s, 3H), 1.66 (s, 3H), 3.31 (d, J(H, P): 27 Hz, 1H), 3.32 (s, 3H), 3.48 (m, 2H), 3.60 (m, 2H), 4.00–4.30 (m, 4H), 7.88 (bs, 1H). ^{31}P NMR ($CDCl_3$, δ, ppm): 28.07. ESI-MS: $[M + H]^+$ = 439, $[M + Na]^+$ = 461. Anal. Calcd for $C_{20}H_{43}N_2O_6P$: C, 54.78%; H, 9.88%; N, 6.39%. Found: C, 54.55%; H, 10.19%; N, 6.38%.

Alkoxyamine 5. BlocBuilder MA (1.0 g, 2.6 mmol), *tert*-butylamine (0.29 g, 4 mmol, 1.5 equiv.), benzotriazol-1-yl-oxytripyrrolidinophosphonium hexafluorophosphate (PyBOP, 2.1 g, 4 mmol, 1.5 equiv.), and DCM (10 mL) were introduced into a round-bottomed flask, and the dispersion was deoxygenated for 20 min by argon bubbling. *N*,*N*-Diisopropylethylamine (DIPEA, 1.35 mL, 7.8 mmol, 3 equiv.) was then added with a syringe through a septum. The mixture was stirred at room temperature for 70 minutes. The DCM was removed under reduced pressure, and the residue was dissolved in ethyl acetate. After filtration over silica gel, ethyl acetate was distilled off and the obtained final product was further dried under vacuum. Yield: 49% (0.57 g). ^{1}H NMR ($CDCl_3$, δ, ppm): 1.16 (s, 9H), 1.18 (s, 9H), 1.33 (m, 6H), 1.37 (s, 9H), 1.55 (s, 3H), 1.63 (s, 3H), 3.33 (d, J(H, P): 27 Hz, 1H), 4.00–4.30 (m, 4H), 6.96 (bs, 1H). ^{31}P NMR ($CDCl_3$, δ, ppm): 26.02. ESI-HRMS: calcd for $C_{21}H_{45}N_2O_5P$ $[M + H]^+$ 437.3139, found 437.3140.

Alkoxyamine 6. BlocBuilder MA (0.5 g, 1.3 mmol), acetylated glucosamine hydrochloride (0.754 g, 2.17 mmol, 1.5 equiv.), PyBOP (1.0 g, 1.92 mmol, 1.5 equiv.), and chloroform (5 mL) were introduced into a round-bottomed flask, and the dispersion was deoxygenated for 20 min by argon bubbling. DIPEA (0.68 mL, 7.42 mmol, 5.5 equiv.) was then added with a syringe through a septum. The mixture was stirred at room temperature for 3.0 h. The mixture was then washed successively with a 5 wt% HCl solution, NaCl-saturated aqueous solution, $NaHCO_3$-saturated solution, NaCl-saturated solution, and finally HCl 5 wt% solution, and then dried on magnesium sulfate, and filtered. After evaporation of chloroform, the product was obtained in 50% yield. ^{1}H NMR ($CDCl_3$, δ, ppm): 7.68–7.17 (dd, 1H), 6.13–6.08 (dd, 1H), 5.38 (m, 1H), 5.12 (m, 1H), 4.58(m, 1H), 4.28–3.95 (m, 7H), 3.29–3.22 (dd, 1H), 2.31–1.96 (m, 12H), 1.68–1.46 (m, 6H), 1.43–1.21 (m, 6H), 1.12–1.08 (m, 18 H). ^{31}P NMR ($CDCl_3$, δ, ppm): 25.82, 25.60.

ESI-HRMS: calcd for $C_{31}H_{55}N_2O_{14}P$ $[M + H]^+$ 711.3464, found 711.3463.

Alkoxyamine 7. Under an inert atmosphere, a solution of SG1 (8.33 mmol, 2.88 g) and 2-bromo-2-methyl-*N*,*N*-dimethylpropanamide (12.5 mmol, 2.425 g) in THF (30 mL) was added to a deoxygenated mixture of CuBr (12.5 mmol, 1.793 g), PMDETA (25.0 mmol, 4.332 g), and Cu(0) (12.5 mmol, 794 mg) in THF (20 mL). After stirring for 24 h at room temperature, the mixture was evaporated, diluted with diethyl oxide and filtered off on Celite. The mixture was then washed successively with a 5 wt% hydrochloric acid (HCl) solution, NaCl-saturated aqueous solution, $NaHCO_3$-saturated solution, NaCl-saturated solution, and finally HCl 5 wt% solution, then dried on magnesium sulfate, and filtered. After evaporation of diethyl ether, the mixture was precipitated in cold pentane to obtain the alkoxyamine as a white powder. Yield: 63%. ^{1}H NMR ($CDCl_3$, δ, ppm): 0.95 (s, 9H), 1.02 (s, 9H), 1.16 (m, 6H), 1.38 (s, 3H), 1.55 (s, 3H), 2.74 (bs, 3H), 3.07 (d, J(H, P): 27 Hz, 1H), 3.31 (bs, 3H), 3.88–4.05 (m, 4H). ^{31}P NMR ($CDCl_3$, δ, ppm): 25.83. ESI-HRMS: calcd for $C_{19}H_{41}N_2O_5P$ $[M + H]^+$ 409.2826, found 409.2827.

Alkoxyamine 9. Under an inert atmosphere, a solution of SG1 (8.33 mmol, 2.88 g) and 2-bromo-*N*,*N*-dimethylpropanamide (12.5 mmol, 2.25 g) in THF (30 mL) was added to a deoxygenated mixture of CuBr (12.5 mmol, 1.793 g), PMDETA (25.0 mmol, 4.332 g), and Cu(0) (12.5 mmol, 794 mg) in THF (20 mL). After stirring for 24 h at room temperature, the mixture was evaporated, diluted with diethyl oxide and filtered off on Celite. The mixture was then washed successively with a 5 wt%. HCl solution, NaCl-saturated aqueous solution, $NaHCO_3$-saturated solution, NaCl-saturated solution, and finally HCl 5 wt% solution, and then dried on magnesium sulfate, and filtered. After evaporation of diethyl ether, the mixture was precipitated in cold pentane to obtain the alkoxyamine as a white powder. Yield: 63%. ^{1}H NMR ($CDCl_3$, δ, ppm): 1.0–1.15 (m, 18H), 1.15–1.25 (m, 6H), 1.28–1.45 (m, 3H), 2.78–2.93 (m, 3H), 2.93–3.10 (m, 3H), 3.14–3.37 (m, 1H), 3.82–4.33 (m, 4H), 4.77–5.10 (m, 1H). ^{31}P NMR ($CDCl_3$, δ, ppm): 24.70, 24.22. ESI-HRMS: calcd for $C_{18}H_{39}N_2O_5P$ $[M + H]^+$ 395.2669, found 395.2670.

Alkoxyamine 10. Under an inert atmosphere, a solution of SG1 (10.3 mmol, 3.165 g) and 2-bromo-*N*-isopropylpropanamide (15.5 mmol, 3.0 g) in THF (30 mL) was added to a deoxygenated mixture of CuBr (15.5 mmol, 2.218 g), PMDETA (31.0 mmol, 5.359 g), and Cu(0) (15.5 mmol, 982 mg) in THF (20 mL). After stirring for 24 h at room temperature, the mixture was evaporated, diluted with diethyl oxide and filtered off on Celite. The mixture was then washed successively with a 5 wt% HCl solution, NaCl-saturated aqueous solution, $NaHCO_3$-saturated solution, NaCl-saturated solution, and finally HCl 5 wt% solution, then dried on magnesium sulfate, and filtered. After evaporation of diethyl ether, the mixture was precipitated in cold pentane to obtain the alkoxyamine as a white powder. Yield: 65%. ^{1}H NMR ($CDCl_3$, δ, ppm): 0.98–1.20 (m, 24H), 1.20–1.31 (m, 6H), 1.33–1.56 (m, 3H), 3.15–3.44 (m, 1H), 3.71–4.51 (m, 6H), 8.0–7.24 (d, 1H). ^{31}P NMR ($CDCl_3$, δ, ppm): 25.91, 25.83. ESI-HRMS: calcd for $C_{19}H_{41}N_2O_5P$ $[M + H]^+$ 409.2826, found 409.2829.

Alkoxyamine 16. A solution of BlocBuilder MA (4.04 g, 10.6 mmol) and *N*-isopropyl acrylamide (1.0 g, 8.84 mmol) in THF was introduced into a Schlenk tube, deoxygenated by nitrogen bubbling and heated at 100 °C for 1 h under stirring. The reaction mixture was then concentrated under reduced pressure. The yellowish oil was dissolved in DCM and washed with water. After drying on magnesium sulfate, filtration and evaporation of DCM, the mixture was precipitated in cold pentane to obtain the alkoxyamine as a white powder. Yield: 57%. ^{1}H NMR ($CDCl_3$, δ, ppm): 1.05–1.40 (m, 36H), 2.07–2.15 (dd, 1H), 2.63–2.67 (dd, 1H), 3.28–3.32 (dd, 1H), 3.96–4.48 (m, 6H), 6.79–6.82 (d, 1H). ^{31}P NMR ($CDCl_3$, δ, ppm): 24.73, 25.03. ESI-HRMS: calcd for $C_{23}H_{47}N_2O_7P$ $[M + H]^+$ 495.3194, found 495.3187.

Determination of the dissociation rate constants (k_d)

Determination by ESR. The time evolution of the doubly integrated ESR signal of the nitroxide radicals was followed by ESR spectroscopy. The appearance of the nitroxides was followed in *tert*-butylbenzene (0.6 mL) containing initially typically a 10^{-4} M solution of alkoxyamines. O_2 was used as a radical scavenger. Samples with known concentrations of nitroxide served as calibration standards.

Determination by ^{31}P NMR. Values of the homolysis rate constant k_d were determined by monitoring the concentration of alkoxyamine by ^{31}P NMR in the presence of the nitroxyl radical TEMPO as an alkyl radicals scavenger during the heating of the corresponding alkoxyamines. A stock solution of 0.02 M of alkoxyamine in *tert*-butylbenzene with 2 equiv. of TEMPO was prepared and sampled in 15 NMR probes (0.5 mL in each probe). They were sunk in a pre-heated oil bath, withdrawn at various time intervals and quenched in an ice-water bath. Then, 0.1 ml of C_6D_6 with $(EtO)_3PO$ (0.002 M) as an internal standard (δ = 0 ppm) were added to each sample. ^{31}P NMR signal was recorded with conventional conditions on a 400 MHz machine.

Polymerization reactions

In all cases, the targeted M_n at 100% monomer conversion was 20 000 g mol^{-1}.

Polymerization of styrene (S). S (2.5 g, 2.40×10^{-2} mol) and the alkoxyamine (AMA (expt. 1): 46.8 mg; AMA-NHS (expt. 2): 59.5 mg; AMA-Gem (expt. 3): 78.5 mg, 1.28×10^{-4} mol) were introduced into a 5 mL vial fitted with a rubber septum and a magnetic bar. The mixture was deoxygenated under stirring by nitrogen bubbling for 15 min at room temperature. The mixture was then immersed in a preheated oil bath at 120 °C, corresponding to time zero of the reaction (according to the small volume of the solution and its quasi-instantaneous heating). Samples were periodically taken to follow S conversion using ^{1}H NMR spectroscopy and the molar mass and dispersity evolutions using SEC. Identical experiments (expts 4–6, respectively) were performed with the addition of 10 mol% free SG1 (3.8 mg, 1.29×10^{-5} mol).

Polymerization of *n*-butyl acrylate (*n*BA). A typical polymerization procedure is as follows. *n*BA (1.0 g, 7.81×10^{-3} mol), alkoxyamine (AMA (expt. 7): 18.5 mg; AMA-NHS (expt. 8): 23.5 mg; AMA-Gem (expt. 9): 30.9 mg, 5.05×10^{-5} mol), free SG1 (1.5 mg, 5.10×10^{-6} mol) and anhydrous toluene (1.0 g, 1.15 mL) were introduced into a 5 mL vial fitted with a rubber septum and a magnetic bar. The mixture was deoxygenated under stirring by nitrogen bubbling for 15 min at room temperature. The mixture was then immersed in a preheated oil bath at 120 °C, corresponding to time zero of the reaction (according to the small volume of solution and its quasi-instantaneous heating). Samples were periodically taken to follow *n*BA conversion using ^{1}H NMR spectroscopy, and the molar mass and dispersity evolutions using SEC.

Copolymerization of methyl methacrylate (MMA) with a small amount of acrylonitrile (AN). Distilled MMA (1.0 g, 1.00×10^{-2} mol), acrylonitrile (AN, 52.5 mg, 9.91×10^{-4} mol), alkoxyamine (AMA (expt. 10): 20.5 mg; AMA-NHS (expt. 11): 25.9 mg; AMA-Gem (expt. 12): 34.2 mg, 5.59×10^{-5} mol), free SG1 (1.6 mg, 5.59×10^{-6} mol) and anhydrous toluene (1.0 g, 1.15 mL) were introduced into a 5 mL vial fitted with a rubber septum and a magnetic bar. The mixture was deoxygenated under stirring by nitrogen bubbling for 15 min at room temperature. The mixture was then immersed in a preheated oil bath at 100 °C, corresponding to time zero of the reaction (according to the small volume of solution and its quasi-instantaneous heating). Samples were periodically taken to follow MMA conversion using ^{1}H NMR spectroscopy, and molar mass and dispersity evolutions using SEC. Identical experiments (expts 13–15) were performed with 15 mol% of AN (93.5 mg, 1.76×10^{-3} mol).

Results and discussion

Synthesis and dissociation behavior of amide-functionalized SG1-based alkoxyamines

A broad library of different SG1-based alkoxyamines was prepared by varying the structure of the amide group and the stabilization of the alkyl moiety (*i.e.*, tertiary or secondary alkyl moiety) (**1–16**, Scheme 3). Alkoxyamine **8** (AMA) was prepared by copper metal-mediated synthesis[22] whereas its *N*-succinimidyl derivative **11** (AMA-NHS) was obtained from AMA by a DCC-assisted coupling reaction with *N*-hydroxysuccinimide.[9] Alkoxyamines **3a** and **3b** were prepared by the reaction of the corresponding *N*-succinimidyl derivatives of the BlocBuilder alkoxyamine **1**.[8] For hindered alkoxyamines **4–6** and **12**, a direct coupling between the parent molecule and the corresponding amine was performed using PyBOP as a coupling agent.[11] The reaction proceeded through the formation of an activated benzatriazole ester of the BlocBuilder under basic conditions, followed by the nucleophilic attack of the amino compound, leading to the desired alkoxyamine in nearly quantitative yields after only 20–30 min (or 24 h for alkoxyamine **12**). Tertiary alkoxyamines **2** and **7** with disubstituted amine moieties were prepared by atom transfer radical addition (ATRA) from the corresponding alkyl bromides.[24,25] Alkoxyamines **13–16** were prepared by 1,2 intermolecular radical addition onto the corresponding olefins.[26] This synthetic route was shown to be very efficient for the preparation of secondary functionalized SG1-based alkoxyamines that can also act as precursors for macromolecular engineering. The penultimate unit effect (PUE) is known to drastically increase the dissociation rate constant of alkoxyamines **13–16** due to the

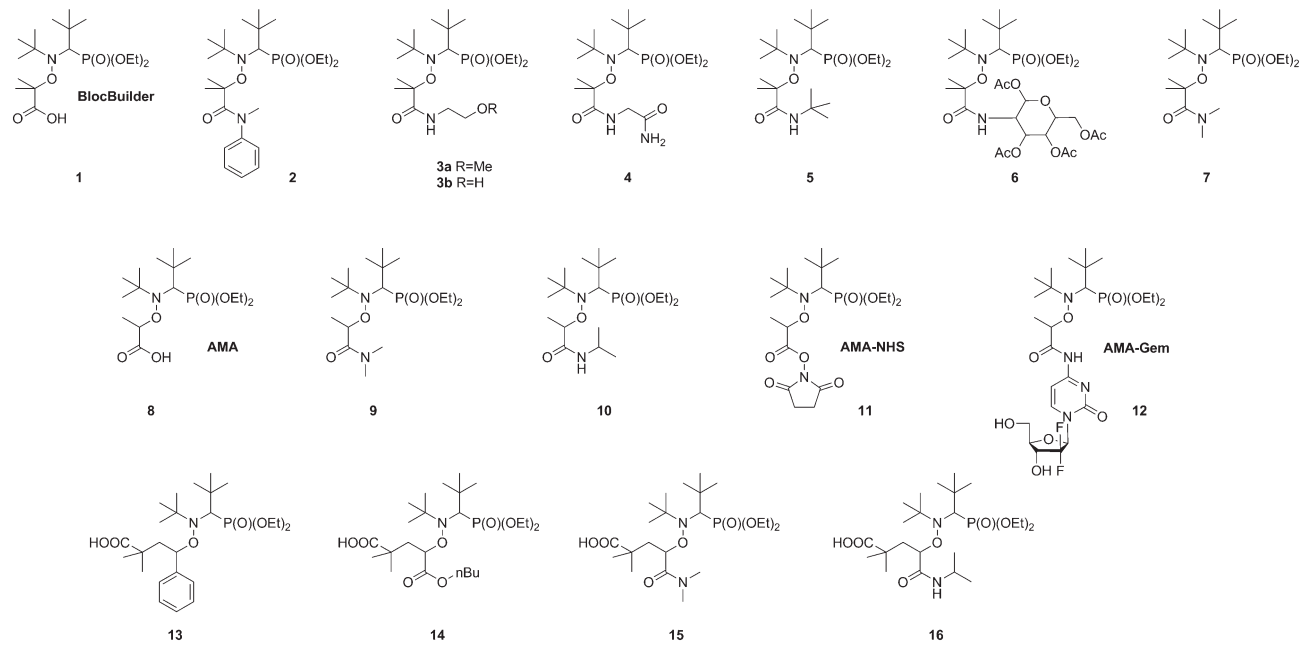

Scheme 3 Structure of the different amide-functionalized SG1-based alkoxyamines synthesized and evaluated in this study.

Table 1 Experimental activation energy of the C–ON bond dissociation for various alkoxyamines

Alkoxyamine	E_a (kJ mol^{-1})	Ref.
1 (BlocBuilder)	112	13
2	105.5[a]	This work
3a	122[b]	This work
3b	125	20
4	117.9[a]	This work
5	123.5[b]	This work
6	121.6[b]	This work
7	112.3[b]	This work
8 (AMA)	130.7/132.8	28
9	124.5[b]	This work
10	135[b]	This work
11 (AMA-NHS)	127.2[b]	This work
12 (AMA-Gem)	131[b]	This work
13	115/116	27
14	124.5	27
15	122.5/123.4	27
16	130[b]	This work

[a] Measured using ^{31}P NMR. [b] Measured using ESR.

presence of the hindered 1-carboxy-1-methyl-ethyl fragment.[27] Therefore, the corresponding secondary SG1-based alkoxyamines **9** and **10** were also prepared with a simple methyl group in place of the 1-carboxy-1-methyl-ethyl fragment from the alkyl halide derivatives by ATRA.[25]

The dissociation rate constant (k_d) measurements were performed either by monitoring the alkoxyamine concentration decay by means of ^{31}P NMR in the presence of an excess of thiophenol as an alkyl radical and a nitroxide scavenger or by monitoring the increase of nitroxide concentration using ESR with oxygen as an alkyl radical scavenger. It has already been shown that k_d values were not significantly different whatever be the techniques used.[28] All experiments were carried out two times and activation energies E_a were estimated using the averaged frequency factor $A = 2.4 \times 10^{14}$ s^{-1}.[29] The results are summarized in Table 1.

To rationalize the reactivity observed with molecules **1–16**, a multi-parameter procedure was applied. This approach was shown to be very robust to describe and emphasize the various effects involved in the C–ON bond homolysis of alkoxyamines. Considering that parameters given in the literature cannot fully describe many alkyl moieties, they were estimated to characterize steric, polar and stabilization effects (see ESI† for details). Experimental k_d values were then plotted against the steric Charton constant ν, the electrical Hammett constants σ_I, and the radical stabilization constants σ_{RS}, representing the steric, polar and stabilization effects, respectively (Fig. 1).

Each experimental log k_d at 120 °C of all alkoxyamines has then been correlated to the steric Charton constant ν, the electrical Hammett constants σ_I, and the radical stabilization constants σ_{RS} parameters to give the best linear relationship (see ESI†). The obtained parameters leading to a linear relationship did not significantly differ from those already reported[29] showing that alkoxyamines **2**, **7**, **9** and **15** behave as expected for SG1-based alkoxyamines. In contrast, alkoxyamines **3–6**, **10**

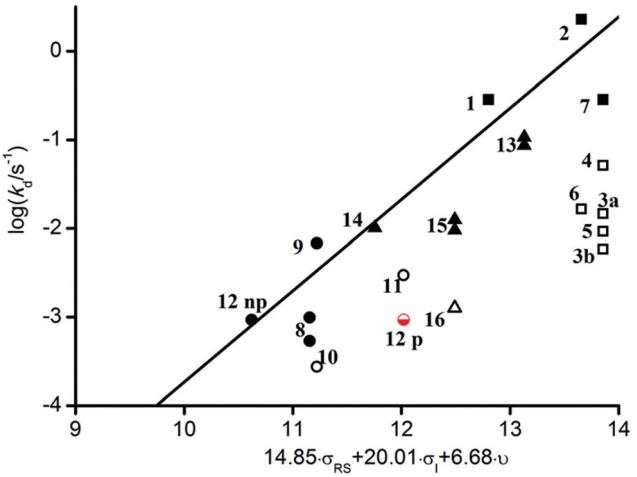

Fig. 1 Plot of log (k_d/s^{-1}) *vs.* the steric Charton constant ν, the electrical Hammett constants σ_I, and the radical stabilization constants σ_{RS} parameters. (■ and □) Tertiary alkoxyamines, (○ and ●) alkoxyamine exhibiting the penultimate unit effect (PUE), and (▲ and △) secondary alkoxyamines. Empty symbols denote outliers. For alkoxyamine **12**, 2 data sets are presented: one with a low polar parameter (**12 np**) and one with a high polar parameter (**12 p**); see text and ESI† for details.

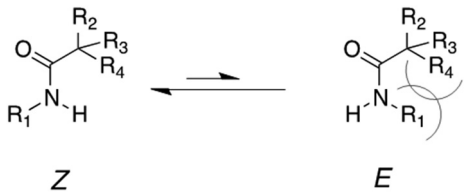

Fig. 2 Structure of the *Z* and *E* diastereoisomer configurations for amide-functionalized SG1-based alkoxyamines. The *E* diastereoisomer is discarded due to the relief of the steric strain.

and **16** exhibited a higher E_a than expected (*ca.* 7–10 kJ mol^{-1}). The main difference between these 2 groups of alkoxyamines comes from the nature of the nitrogen in the amide function (*i.e.*, disubstituted for the former and monosubstituted for the latter). It is known that long-range steric or polar effects arose for SG1-based alkoxyamines bearing different ester chains. Nevertheless in the case of amide bonds, similar unusual behaviours reported for alkoxyamines **3–6** denote that the type of alkyl groups has a marginal influence on E_a, as opposed to ester-functionalized analogues. This reactivity could be ascribed to the predominance of the *Z* diastereoisomer configuration which is favoured due to the relief of steric strain (Fig. 2).

The *Z* configuration with the hydrogen atom pointing towards the nitroxide moiety could also explain the decreased lability of alkoxyamines bearing a monosubstituted nitrogen on the amide function. It might indeed induce some intramolecular hydrogen-bonding (IHB) between the alkyl and the nitroxide fragments, which generates a new bond to cleave, hence increasing the activation energy. The predominance of the

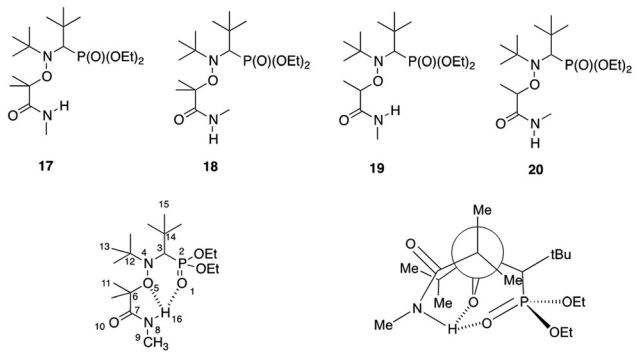

Scheme 4 Structures of the calculated amide-functionalized alkoxyamines and representation of the multiple intramolecular hydrogen-bonding interactions.

Z isomer configuration was assessed by X-ray analysis of alkoxyamine **3b** (see ESI†). As for alkoxyamines **3–6**, only one peak was observed by ^{31}P NMR in the crude materials. Based on **3b**, it was assumed that all these alkoxyamines exhibited the *Z* configuration. The IHB interaction was then studied by DFT calculations on a selection of representative model alkoxyamines **17** and **19** (IHB capable) and **18** and **20** (not IHB capable) (Scheme 4). DFT optimized structures of **3b** and **1** (BlocBuilder) were very close to their corresponding X-ray structures (see ESI† for details), demonstrating that the level of theory applied was suitable. The calculated bond distances are summarized in ESI† and showed that, whatever the alkyl moieties, all nitroxide fragments exhibited close conformations. Multi-IHB between the hydrogen on the amide group and the oxygens of the nitroxide was highlighted by the bond distances in alkoxyamine **17**, giving $d_{H16\cdots O5}$ = 2.101 Å and $d_{H16\cdots O1}$ = 2.586 Å. In both cases, these values were smaller than the sum of the van der Waals radii of H atoms and oxygen atoms (r_H = 1.34 Å, r_O = 1.68 Å, and Σ_{vdW} = 3.02 Å). The value for the valence angle $<N_8H_{16}O_1>$ (larger than 170°) highlighted a strong IHB whereas the value of 106° for $<N_8H_{16}O_5>$ gave a weak to moderate IHB (Scheme 4). Note that a weak to moderate IHB has already been reported for BlocBuilder MA alkoxyamine[30,31] as well as for a SG1-based alkoxyamine carrying hydroxyl group on the alkyl moiety.[32,33]

In conclusion, the establishment of IHB increasing the dissociation energy by *ca.* 7–10 kJ mol^{-1} for a series of monosubstituted amide-functionalized SG1-based alkoxyamines has been evidenced. The situation for AMA-Gem **12** is however more complex since the estimation of its polar parameter cannot be performed (the value for the cytosine group is not reported). We used the polarity value of the model phenyl ring in the first approximation and the predicted dissociation behavior fulfilled the linear relationship already reported for SG1-based alkoxyamines (**12np** in Fig. 1). Nevertheless, as the cytosine moiety should be prone to IHB, a higher activation was expected. A better estimation was then performed using an oxopyrimidinyl group (**12p** in Fig. 1). As expected for such an alkoxyamine, the activation energy was increased by *ca.* 10 kJ mol^{-1}, due to the occurrence of IHB.

The experimental activation energy of **12** (E_a = 131 kJ mol^{-1}) was similar to that of the acid-functionalized analogue (E_a = 130/132 kJ mol^{-1} for the diastereoisomers). This value was lower than that of alkoxyamine **10** (E_a = 135 kJ mol^{-1}), a model of amide-functionalized SG1-based alkoxyamine, and was similar to the reference MONAMS alkoxyamine.[34] In the case of AMA-Gem **12**, the influence of IHB over the dissociation was entirely counter-balanced by the presence of the polar cytosine ring on the amide function that promoted the dissociation.

The aim of the next section was therefore to estimate its performance in NMP in comparison with two precursors of amide-functionalized alkoxyamines, namely the acid-functionalized AMA alkoxyamine and its NHS derivative (AMA-NHS).

NMP of vinyl monomers initiated by different SG1-based alkoxyamines

NMP of styrene (S). The bulk polymerization of S at 120 °C was investigated, as it is one of the most widely-used monomers in radical polymerization. Experiments were first performed without any addition of free SG1 (expts 1–3). First-order kinetics were obtained up to 50–80% monomer conversion for the three alkoxyamines tested (Fig. 3a), accounting for a constant concentration of propagating radicals during the polymerizations. Although molar masses increased linearly in all cases, some differences were highlighted. AMA-NHS led to the higher polymerization rate (Fig. 3a), whereas a low apparent initiation efficiency (calculated according to f = theoretical M_n/experimental M_n) of ~60% was obtained with AMA, compared to ~80% for AMA-NHS and AMA-Gem (Fig. 3b). Also, AMA-NHS led to low dispersities ($Đ$ ~1.2) compared to AMA and AMA-Gem, for which dispersities approached 1.5 at the end of the polymerization. This latter observation was likely attributed to the higher dissociation rate constant of AMA-NHS (Table 1), which is known to be a key parameter to achieve good control of the NMP process.[14]

The situation was however less marked by adding 10 mol% of free SG1 at the onset of the polymerizations (expts 4–6, Fig. 4). This drastically reduced the differences of behavior between the three alkoxyamines as: (i) kinetics rather exhibited the same slope (Fig. 4a); (ii) the initiation efficiency was greatly improved for AMA (expt. 4, Fig. 4b) with M_n values almost overlapping with those obtained from AMA-Gem and AMA-NHS and (iii) dispersities reached lower values for AMA and AMA-Gem ($Đ$ ~1.4), and so was for AMA-NHS ($Đ$ ~1.15). The presence of 10 mol% of free SG1 at the very beginning of the polymerization helped in reducing the occurrence of irreversible terminations and therefore reduced the differences between the dissociation abilities of these three alkoxyamines.

NMP of *n*-butyl acrylate (*n*BA). SG1 is an efficient controlling agent for the polymerization of a broad variety of different acrylic esters.[1] A representative acrylic ester that is often polymerized by NMP is *n*BA. Many studies have reported the SG1-mediated polymerization of *n*BA under many different conditions.[35–38] NMP was performed at 120 °C in the presence

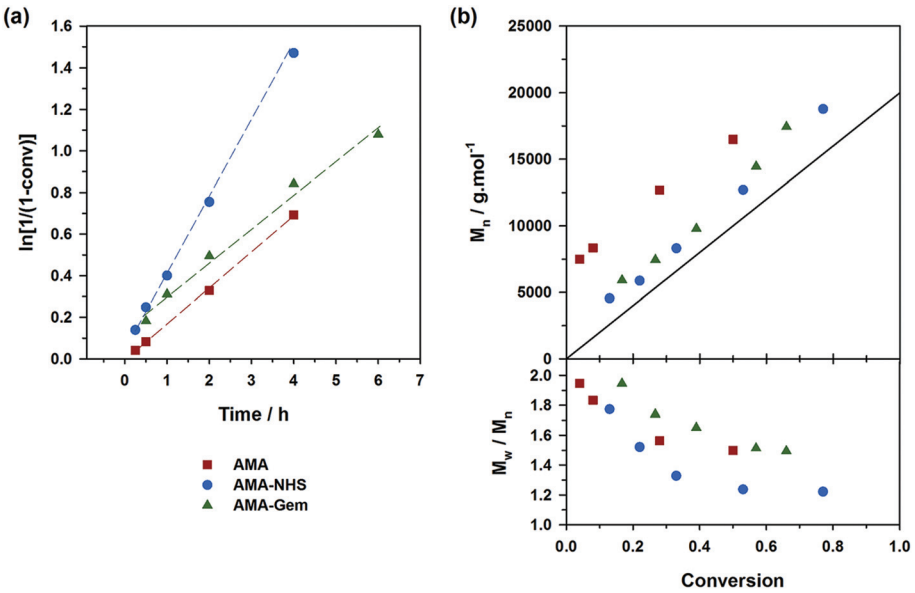

Fig. 3 Bulk NMP of S at 120 °C initiated by different SG1-based alkoxyamines: ■, expt. 1 (AMA); ●, expt. 2 (AMA-NHS); ▲, expt. 3 (AMA-Gem). (a) Evolution of ln[1/(1 – conv.)] with time (t); (b) evolution of the number-average molar mass (M_n) and dispersity ($Đ$) with conv. The full lines represent the theoretical M_n and lines connecting data points are only guide for the eye.

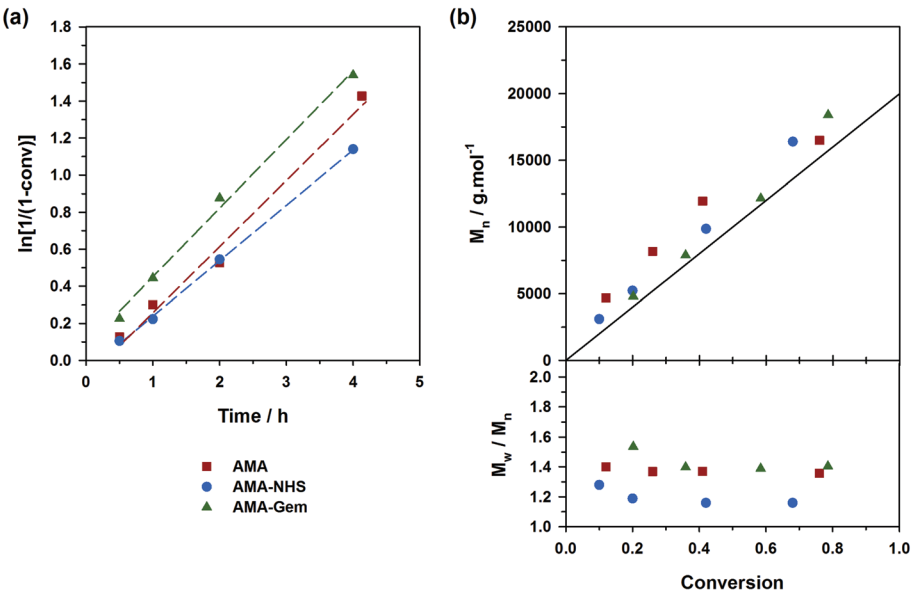

Fig. 4 Bulk NMP of S at 120 °C initiated by different SG1-based alkoxyamines in the presence of 10 mol% free SG1: ■, expt. 4 (AMA); ●, expt. 5 (AMA-NHS); ▲, expt. 6 (AMA-Gem). (a) Evolution of ln[1/(1 – conv.)] with time (t); (b) evolution of the number-average molar mass (M_n) and dispersity ($Đ$) with conv. The full lines represent the theoretical M_n and lines connecting data points are only guide for the eye.

of 10 mol% of free SG1 (expts 7–9, Fig. 5). A small amount of free SG1 is indeed mandatory to efficiently control the polymerization of *n*BA, especially initiated by secondary SG1-based alkoxyamines.[36] For the three alkoxyamines, not so much difference was observed. As expected, AMA-NHS gave the highest polymerization rate (Fig. 5a) but the quality of control was identical whatever the nature of the alkoxyamine (Fig. 5b). M_n values linearly increased during the polymerization with high initiating efficiencies and decreasing dispersities ($Đ$ ~1.35) up to 70% *n*BA conversion. As expected, dispersities increased above 80% *n*BA conversion due to side reactions such as chain transfer to a polymer.[39,40]

NMP of methyl methacrylate (MMA). NMP of MMA and methacrylates, in general, has always been challenging.[41] Using SG1 as a controlling agent results in a high activation–deactivation equilibrium rate constant that favors the pro-

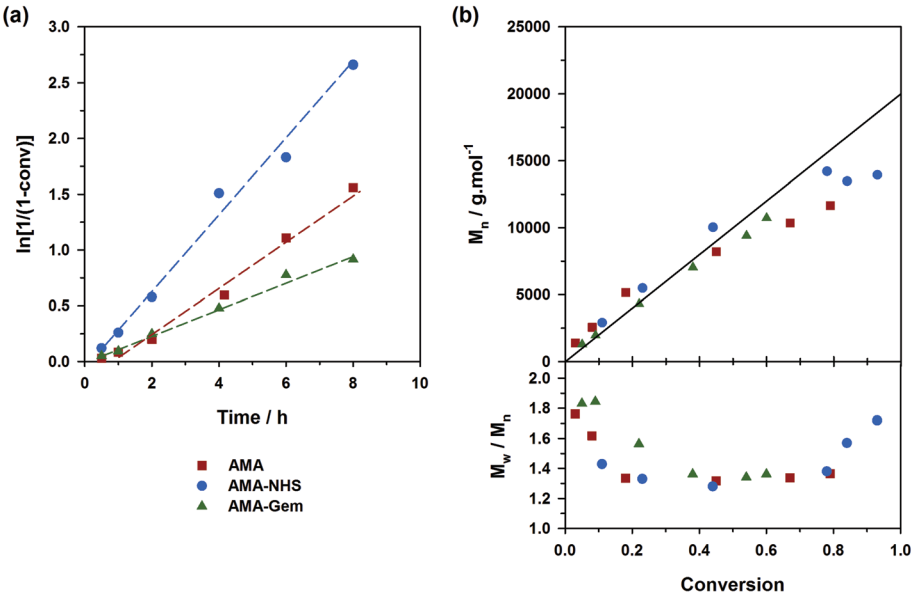

Fig. 5 Solution NMP of *n*BA at 120 °C initiated by different SG1-based alkoxyamines: ■, expt. 7 (AMA); ●, expt. 8 (AMA-NHS); ▲, expt. 9 (AMA-Gem). (a) Evolution of ln[1/(1 − conv.)] with time (t); (b) evolution of the number-average molar mass (M_n) and dispersity ($Đ$) with conv. The full lines represent the theoretical M_n and lines connecting data points are only guide for the eye.

duction of propagating radicals.[42,43] This leads to a high level of irreversible termination reactions (both homotermination between propagating radicals and β-hydrogen transfer from the propagating radical to the nitroxide).[43–46] The polymerization is therefore rapidly stopped and polymers with high dispersities and low molar masses are obtained. However, the addition of a small amount of S during the SG1-mediated polymerization of MMA, initiated with a high dissociation rate constant alkoxyamine such as BlocBuilder, enabled well-defined and living polymers to be readily synthesized due to

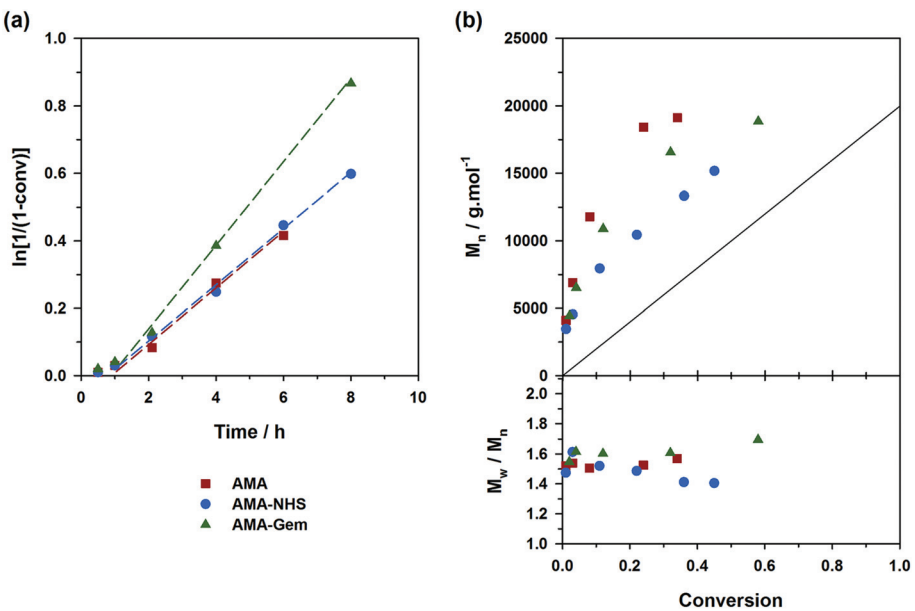

Fig. 6 Solution NMP of methyl methacrylate (MMA) with a small amount of acrylonitrile (AN, f_{AN0} = 9 mol%) at 100 °C initiated by different SG1-based alkoxyamines: ■, expt. 10 (AMA); ●, expt. 11 (AMA-NHS); ▲, expt. 12 (AMA-Gem). (a) Evolution of ln[1/(1 − conv.)] with time (t); (b) evolution of the number-average molar mass (M_n) and dispersity ($Đ$) with conv. The full lines represent the theoretical M_n and lines connecting data points are only guide for the eye.

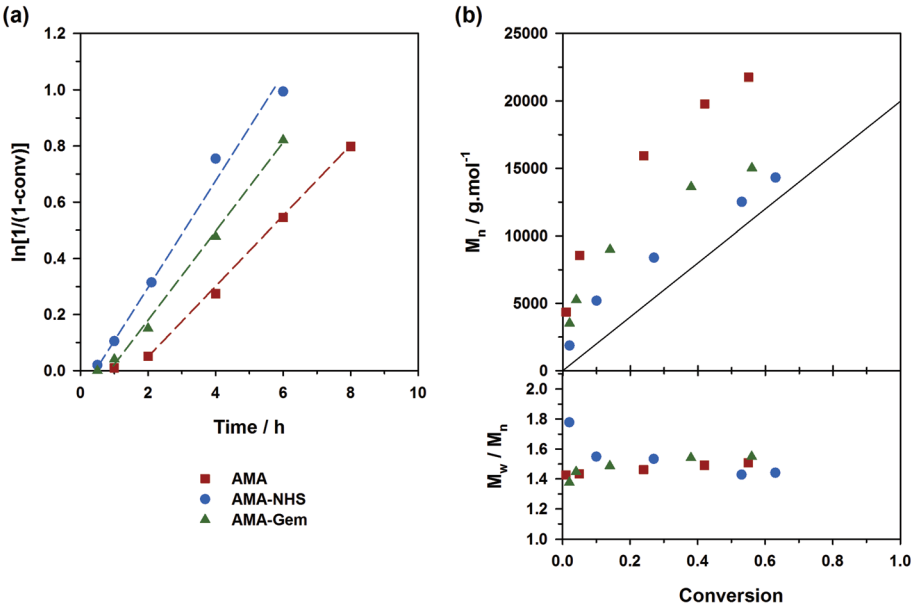

Fig. 7 Solution NMP of methyl methacrylate (MMA) with a small amount of acrylonitrile (AN, f_{AN0} = 15 mol%) at 100 °C initiated by different SG1-based alkoxyamines in the presence of 10 mol% free SG1: ■, expt. 13 (AMA); ●, expt. 14 (AMA-NHS); ▲, expt. 15 (AMA-Gem). (a) Evolution of ln[1/(1 – conv.)] with time (t); (b) evolution of the number-average molar mass (M_n) and dispersity ($Đ$) with conv. The full lines represent the theoretical M_n and lines connecting data points are only guide for the eye.

the drastic decrease of the average activation–deactivation equilibrium rate constant, $\langle K \rangle$.[45,47] This was attributed to favorable kinetic parameters of S (*i.e.*, low K and low cross-propagation rate constant).[45,48] This strategy is versatile as it can be extended to other methacrylic esters[49–54] and other 'controlling' comonomers such as acrylonitrile (AN)[55] and 9-(4-vinylbenzyl)-9*H*-carbazole (VBK).[56]

Controlling the NMP of MMA with secondary alkoxyamines is therefore not straightforward due to their slower decomposition rates compared to their tertiary analogues. Polymerizations were performed at 100 °C (and not at 90 °C to alleviate the detrimental effect of their relatively high E_a) in the presence of 9 mol% of AN (expts 10–12, Fig. 6). Results showed a substantially better control with AMA-NHS compared to AMA and AMA-Gem. With AMA-NHS, M_n values were closer to the predicted ones (indicating a higher initiation efficiency, although quite modest as f = 60%) and dispersities progressively decreased to ~ 1.4. In contrast, although M_n values were still increasing linearly with MMA conversion for AMA and AMA-Gem up to *ca.* 30% conversion, significantly higher dispersities ($Đ$ ~1.6–1.7) were obtained during the polymerization. This particular case, for which a fast-dissociating alkoxyamine is necessary, highlighted the pivotal role of the k_d value in the control of the NMP process and exalted the difference between the behaviors of the three alkoxyamines.

A strategy to improve the control is to slightly increase the initial amount of the 'controlling' comonomer, while still targeting low values to maintain a high amount of methacrylic units in the resulting copolymer. By using f_{AN0} = 15 mol%, a significant improvement was indeed witnessed (expts 13–15, Fig. 7). Whereas similar first-order kinetics were observed in all cases, AMA-NHS and AMA-Gem led to higher initiation efficiencies (f = 89% and 75%, respectively) whereas that of AMA was rather unchanged and still poor. Also, dispersities for AMA and AMA-Gem were slightly improved and reached lower values at the end of the polymerization ($Đ$ ~1.5), compared to similar experiments with 9 mol% AN (see Fig. 6b). However, no beneficial effect on the dispersity was observed with AMA-NHS (expt. 14).

General discussion

What resulted from this series of polymerizations with different monomers is overall good agreement between the controlling ability of each alkoxyamine tested (*i.e.*, AMA, AMA-NHS and AMA-Gem) and the value of their activation energy (and implicitly of their dissociation rate constant). AMA-NHS, which exhibits the lowest E_a by *ca.* 4–5 kJ mol^{-1}, indeed led to a better control than AMA and AMA-Gem in terms of initiation efficiency and dispersity, although differences were quite moderate. The addition of a small amount of free SG1 (10 mol%) had the beneficial effect of reducing these differences and improving the control. A similar effect was observed on the MMA polymerization by increasing the amount of controlling comonomer (f_{AN0} = 15 mol% *vs.* 9 mol%).

Despite the establishment of IHB for AMA-Gem, the presence of the polar cytosine ring on the amide function, which favors the dissociation, enabled a fair control of different monomer families. In fact, the initiation efficiency of

AMA-Gem was slightly better than the AMA alkoxyamine, although they exhibited very close E_a. This result could be explained by a higher rate of decomposition during the polymerization process. The occurrence of IHB is indeed likely prone to vary with the polarity of the solvent (without IHB, the dissociation of AMA-Gem would be dramatically increased with a theoretical E_a = 121 kJ mol^{-1}, see ESI† for details), as recently observed for the NMP of isoprene.[31] Note that the nature of the solvent can also impact the alkoxyamine reactivity.[57,58]

Importantly, it appears that when the '*grafting from*' strategy is envisioned from NHS- or COOH-containing AMA-based alkoxyamines, the coupling with a polar amine moiety may still allow the synthesis of well-defined polymers (*i.e.*, IHB will be counter-balanced). In contrast, when a non-polar amine group is envisioned, IHB might reach its maximum value and lead to a significantly higher E_a, thus impacting the quality of control. In this case, the coupling of a preformed polymer could be the preferable pathway toward well-defined functionalized materials. Further investigations are therefore necessary to assess this hypothesis by probing the influence of the polarity of the amine group on the quality of the control.

Conclusion

In this article, a series of different amide-functionalized alkoxyamines (which is a functionality often obtained after conjugation from COOH- or NHS-containing alkoxyamines) based on the nitroxide SG1 have been synthesized and their k_d have been determined. A multi-parameter procedure was applied to rationalize their reactivity. It enabled to discriminate disubstituted alkoxyamines from monosubstituted ones. Whereas disubstituted alkoxyamines displayed expected dissociation abilities for SG1-based alkoxyamines, monosubstituted counterparts exhibited lower k_d (E_a increase of ~7–10 kJ mol^{-1}) because of the occurrence of IHB between the alkyl and the nitroxide fragments. To probe potential consequences on the synthesis of functionalized materials, S, *n*BA and MMA with a small amount of AN were successfully polymerized by NMP from AMA and AMA-NHS, which are two representative secondary SG1-based alkoxyamines employed for conjugation, displaying a carboxylic acid and a NHS group, respectively. Their performances were compared to those of AMA-Gem, a prefunctionalized alkoxyamine subjected to IHB bearing an anticancer drug as a functional moiety *via* an amide bond. It resulted that the strong polarity of the Gem moiety still enabled a fair control despite the detrimental effect of IHB over its k_d. Overall, this work may have important consequences on the design of polymer conjugates from functional alkoxyamines and help in determining the most suitable approach for their design.

Acknowledgements

We thank the French Ministry of Research for the financial support of the PhD thesis of EG and the French National Research Agency (ANR-11-JS08-0005) for the financial support of the PhD thesis of VD. Arkema is warmly acknowledged for kindly providing the BlocBuilder MA™ alkoxyamine and the SG1 nitroxide. The CNRS is also acknowledged for financial support.

Notes and references

1 J. Nicolas, Y. Guillaneuf, C. Lefay, D. Bertin, D. Gigmes and B. Charleux, *Prog. Polym. Sci.*, 2013, **38**, 63–235.
2 R. B. Grubbs, *Polym. Rev.*, 2011, **51**, 104–137.
3 K. Matyjaszewski and J. Xia, *Chem. Rev.*, 2001, **101**, 2921–2990.
4 M. Kamigaito, T. Ando and M. Sawamoto, *Chem. Rev.*, 2001, **101**, 3689–3745.
5 G. Moad, E. Rizzardo and S. H. Thang, *Aust. J. Chem.*, 2009, **62**, 1402–1472.
6 S. Perrier and P. Takolpuckdee, *J. Polym. Sci., Part A: Polym. Chem.*, 2005, **43**, 5347–5393.
7 A. Goto and T. Fukuda, *Prog. Polym. Sci.*, 2004, **29**, 329–385.
8 J. Vinas, N. Chagneux, D. Gigmes, T. Trimaille, A. Favier and D. Bertin, *Polymer*, 2008, **49**, 3639–3647.
9 M. Chenal, C. Boursier, Y. Guillaneuf, M. Taverna, P. Couvreur and J. Nicolas, *Polym. Chem.*, 2011, **2**, 1523–1530.
10 J. Parvole, L. Ahrens, H. Blas, J. Vinas, C. Boissiere, C. Sanchez, M. Save and B. Charleux, *J. Polym. Sci., Part A: Polym. Chem.*, 2010, **48**, 173–185.
11 T. Trimaille, K. Mabrouk, V. Monnier, L. Charles, D. Bertin and D. Gigmes, *Macromolecules*, 2010, **43**, 4864–4870.
12 S. Harrisson, J. Nicolas, A. Maksimenko, D. T. Bui, J. Mougin and P. Couvreur, *Angew. Chem., Int. Ed.*, 2013, **52**, 1678–1682.
13 D. Bertin, D. Gigmes, S. R. A. Marque and P. Tordo, *Macromolecules*, 2005, **38**, 2638–2650.
14 F. Chauvin, P.-E. Dufils, D. Gigmes, Y. Guillaneuf, S. R. A. Marque, P. Tordo and D. Bertin, *Macromolecules*, 2006, **39**, 5238–5250.
15 D. Gigmes, J. Vinas, N. Chagneux, C. Lefay, T. N. T. Phan, T. Trimaille, P.-E. Dufils, Y. Guillaneuf, G. Carrot, F. Boue and D. Bertin, *ACS Symp. Ser.*, 2009, **1024**, 245–262.
16 J. Klein and D. Herzog, *Makromol. Chem.*, 1987, **188**, 1217–1232.
17 W. E. Weaver and W. M. Whaley, *J. Am. Chem. Soc.*, 1947, **69**, 1144–1145.
18 T. Hama, D. A. Culkin and J. F. Hartwig, *J. Am. Chem. Soc.*, 2006, **128**, 4976–4985.
19 C. Leroi, D. Bertin, P.-E. Dufils, D. Gigmes, S. Marque, P. Tordo, J.-L. Couturier, O. Guerret and M. A. Ciufolini, *Org. Lett.*, 2003, **5**, 4943–4945.
20 N. Chagneux, T. Trimaille, M. Rollet, E. Beaudoin, P. Gerard, D. Bertin and D. Gigmes, *Macromolecules*, 2009, **42**, 9435–9442.

21 P.-E. Dufils, N. Chagneux, D. Gigmes, T. Trimaille, S. R. A. Marque, D. Bertin and P. Tordo, *Polymer*, 2007, **48**, 5219–5225.
22 S. Harrisson, P. Couvreur and J. Nicolas, *Polym. Chem.*, 2011, **2**, 1859–1865.
23 The PS calibration is appropriate for PnBA samples as shown by the Mark–Houwink–Sakurada parameters: actually, it leads to an error of about 3–5%, which is within the accepted range for SEC analysis. Indeed, the MHS parameters in THF at 30 °C are the following: $K_{PS} = 11.4 \times 10^{-5}$ dL g^{-1} and $\alpha_{PS} = 0.716$ for PS [see: R. A. Hutchinson, D. A. Paquet Jr., J. H. McMinn, S. Beuermann, R. E. Fuller and C. Jackson, *Dechema Monogr.*, 1995, **131**, 467]; $K_{PnBA} = 12.2 \times 10^{-5}$ dL g^{-1} and $\alpha_{PnBA} = 0.700$ for PnBA [see: S. Beuermann, D. A. Paquet Jr., J. H. McMinn and R. A. Hutchinson, *Macromolecules*, 1997, **29**, 1918].
24 K. Matyjaszewski, B. E. Woodworth, X. Zhang, S. G. Gaynor and Z. Metzner, *Macromolecules*, 1998, **31**, 5955.
25 D. Bertin, D. Gigmes, C. LeMercier, S. R. A. Marque and P. Tordo, *J. Org. Chem.*, 2004, **69**, 4925–4930.
26 D. Gigmes, P.-E. Dufils, D. Gle, D. Bertin, C. Lefay and Y. Guillaneuf, *Polym. Chem.*, 2011, **2**, 1624–1631.
27 D. Bertin, P.-E. Dufils, I. Durand, D. Gigmes, B. Giovanetti, Y. Guillaneuf, S. R. A. Marque, T. Phan and P. Tordo, *Macromol. Chem. Phys.*, 2008, **209**, 220–224.
28 D. Bertin, D. Gigmes, S. Marque and P. Tordo, *e-Polymers*, 2003, **002**, 1–9.
29 D. Bertin, D. Gigmes, S. R. A. Marque and P. Tordo, *Chem. Soc. Rev.*, 2011, **40**, 2189–2198.
30 S. Harrisson, P. Couvreur and J. Nicolas, *Macromolecules*, 2011, **44**, 9230–9238.
31 S. Harrisson, P. Couvreur and J. Nicolas, *Macromol. Rapid Commun.*, 2012, **33**, 805–810.
32 E. G. Bagryanskaya, P. Brémond, T. Butscher, S. R. A. Marque, D. Parkhomenko, V. Roubaud, D. Siri and S. Viel, *Macromol. Chem. Phys.*, 2014, **216**, 475–488.
33 P. Brémond, T. Butscher, V. Roubaud, D. Siri and S. Viel, *J. Org. Chem.*, 2013, **78**, 10524–10529.
34 S. Marque, C. Le Mercier, P. Tordo and H. Fischer, *Macromolecules*, 2000, **33**, 4403–4410.
35 C. Farcet, J. Nicolas and B. Charleux, *J. Polym. Sci., Part A: Polym. Chem.*, 2002, **40**, 4410–4420.
36 P. Lacroix-Desmazes, J.-F. Lutz, F. Chauvin, R. Severac and B. Boutevin, *Macromolecules*, 2001, **34**, 8866–8871.
37 J. Nicolas, B. Charleux, O. Guerret and S. Magnet, *Angew. Chem., Int. Ed.*, 2004, **43**, 6186–6189.
38 J. Nicolas, B. Charleux and S. Magnet, *J. Polym. Sci., Part A: Polym. Chem.*, 2006, **44**, 4142–4153.
39 C. Farcet, J. Belleney, B. Charleux and R. Pirri, *Macromolecules*, 2002, **35**, 4912–4918.
40 Y. Guillaneuf, D. Gigmes and T. Junkers, *Macromolecules*, 2012, **45**, 5371–5378.
41 E. Guégain, Y. Guillaneuf and J. Nicolas, *Macromol. Rapid Commun.*, 2015, accepted.
42 G. S. Ananchenko, M. Souaille, H. Fischer, C. Le Mercier and P. Tordo, *J. Polym. Sci., Part A: Polym. Chem.*, 2002, **40**, 3264–3283.
43 Y. Guillaneuf, D. Gigmes, S. R. A. Marque, P. Tordo and D. Bertin, *Macromol. Chem. Phys.*, 2006, **207**, 1278–1288.
44 C. Dire, J. Belleney, J. Nicolas, D. Bertin, S. Magnet and B. Charleux, *J. Polym. Sci., Part A: Polym. Chem.*, 2008, **46**, 6333–6345.
45 B. Charleux, J. Nicolas and O. Guerret, *Macromolecules*, 2005, **38**, 5485–5492.
46 R. McHale, F. Aldabbagh and P. B. Zetterlund, *J. Polym. Sci., Part A: Polym. Chem.*, 2007, **45**, 2194–2203.
47 J. Nicolas, C. Dire, L. Mueller, J. Belleney, B. Charleux, S. R. A. Marque, D. Bertin, S. Magnet and L. Couvreur, *Macromolecules*, 2006, **39**, 8274–8282.
48 J. Nicolas, L. Mueller, C. Dire, K. Matyjaszewski and B. Charleux, *Macromolecules*, 2009, **42**, 4470–4478.
49 J. Nicolas, P. Couvreur and B. Charleux, *Macromolecules*, 2008, **41**, 3758–3761.
50 B. Lessard and M. Maric, *J. Polym. Sci., Part A: Polym. Chem.*, 2009, **47**, 2574–2588.
51 B. Lessard and M. Marić, *J. Polym. Sci., Part A: Polym. Chem.*, 2011, **49**, 5270–5283.
52 B. Lessard, C. Tervo, S. De Wahl, F. J. Clerveaux, K. K. Tang, S. Yasmine, S. Andjelic, A. D'Alessandro and M. Maric, *Macromolecules*, 2010, **43**, 868–878.
53 B. H. Lessard, E. J. Y. Ling and M. Marić, *Macromolecules*, 2012, **45**, 1879–1891.
54 S. R. S. Ting, E.-H. Min, P. Escale, M. Save, L. Billon and M. H. Stenzel, *Macromolecules*, 2009, **42**, 9422–9434.
55 J. Nicolas, S. Brusseau and B. Charleux, *J. Polym. Sci., Part A: Polym. Chem.*, 2010, **48**, 34–47.
56 B. Lessard, E. J. Y. Ling, M. S. T. Morin and M. Marić, *J. Polym. Sci., Part A: Polym. Chem.*, 2011, **49**, 1033–1045.
57 G. Audran, P. Bremond, S. R. A. Marque and G. Obame, *Polym. Chem.*, 2012, **3**, 2901–2908.
58 G. Audran, P. Brémond, S. R. A. Marque and G. Obame, *J. Org. Chem.*, 2012, **77**, 9634–9640.

